ELSEVIER

Soil Dynamics and Earthquake Engineering 24 (2004) 689–698

SOIL DYNAMICS AND EARTHQUAKE ENGINEERING

www.elsevier.com/locate/soildyn

The use of MASW method in the assessment of soil liquefaction potential

Chih-Ping Lin*, Cheng-Chou Chang, Tzong-Sheng Chang

Department of Civil Engineering, National Chiao Tung University, 1001Ta-Hsueh Road, Hsinchu, Taiwan, ROC

Abstract

The multi-channel analysis of surface wave (MASW) method is a non-invasive method recently developed to estimate shear wave velocity profile from surface wave energy. Unlike conventional SASW method, multi-station recording permits a single survey of a broad depth range and high levels of redundancy with a single field configuration. An efficient and unified wavefield transform technique is introduced for dispersion analysis and on site data quality control. The technique was demonstrated in the assessment of soil liquefaction potential at a site in Yuan Lin, Taiwan. The shear wave velocity and liquefaction potential assessments based on MASW method compares favorable to that based on SCPT shear wave measurements. Two-dimensional shear wave velocity profiles were estimated by occupying successive geophone spreads at several sites in central western Taiwan, at some of which sand boils or ground cracks occurred during 1999 Chi Chi earthquake. Liquefaction potential analysis based on MASW imaging was shown to be effective for estimating the extent of potential liquefaction hazard.

Keywords: Surface wave; Shear-wave velocity; Liquefaction

1. Introduction

The liquefaction resistance of a soil layer can be determined through either laboratory tests on undisturbed soil samples or from in situ tests. Because the cost of collecting undisturbed samples is considerable and the laboratory conditions cannot accurately simulate actual field conditions, the 'simplified procedure' widely used for evaluating soil liquefaction resistance is based on in situ testing methods. Four field tests are recommended in the NCEER workshop for routine evaluation of liquefaction resistance using the 'simplified procedure'—the cone penetration test (CPT), the standard penetration test (SPT), shear-wave velocity (V_S) measurements (SWV), and for gravelly sites the Becker penetration test [1]. Among these testing methods, the SWV technique is most appealing because: (1) the existence of large particles in the soil column (e.g. gravelly soils) that makes penetration tests unreliable has little effect on the shear wave technique, (2) (V_S) can be measured both in the laboratory and in the field, allowing direct comparisons between laboratory and field behavior, (3) (V_S) can be measured by non-destructive surface seismic methods, and (4) (V_S) is directly related to the small-strain shear modulus G_{max}, a required property for predicting the ground motion response to earthquake in areas where significant soil cover exists over firm bedrock [2,3].

The shear wave velocity can be measured using a suite of surface (non-invasive) and borehole (invasive) seismic methods. At shallow depths where liquefaction is of concern, surface seismic methods are attractive since they are non-invasive and relatively inexpensive. Such techniques are effective for 'first look' or reconnaissance investigations where the objective is to ascertain the presence or absence of lateral variations of shear wave structure or to establish average velocity–depth profiles. Non-invasive methods for measuring shear wave velocity include shear wave refraction survey and surface wave methods. Refraction techniques for near surface survey are traditionally based on head-wave methods, which have been well described in the literature [4]. Recent developments in refraction tomography have enhanced the spatial resolution of the refraction survey [5]. However, the results are subject to limitation that velocity must increase with depth. Furthermore, S-wave refraction survey may not provide the true S-wave velocity because of wave-type conversion in an area of non-horizontal layers [6]. Surface wave methods do not suffer from aforementioned problems associated with refraction survey, hence are considered of special interest for the site surveys of liquefaction potential.

Surface wave tests are based on the dispersive nature of Rayleigh waves in vertically heterogeneous media [7–9]. The variation of Rayleigh wave phase velocities with

* Corresponding author. Tel.: +886-3-513-1574; fax: +886-3-571-6257.
E-mail address: cplin@mail.nctu.edu.tw (C.-P. Lin).

0267-7261/$ - see front matter © 2004 Elsevier Ltd. All rights reserved.
doi:10.1016/j.soildyn.2004.06.012

frequency results from the variation of shear wave velocities with depth. The dispersion curve is experimentally determined from the wave field data related to the propagation of a perturbation generated by a dynamic source and recorded by geophones or accelerometers on the ground surface. A subsequent inversion process, based on the numerical simulation of wave propagation in layered media, leads to an estimate of the S-wave velocity profile.

Surface wave tests in geotechnical engineering have been for a long time associated to the two-station set-up used in the SASW test, introduced during the 1980s by the research group at the University of Texas at Austin [7–9]. Despite the attractive feature of the surface wave technique, it is seldom used for site surveys of liquefaction potential. A few weaknesses of the SASW method become obvious in practice. These weaknesses hinder the surface wave method from being widely adopted in practice. The development of the SASW method began with multiple, two-station set-ups and has progressed to multiple-station set-ups with the development of more sophisticated data acquisition systems. For example, Nazarian et al. [10] have developed a trailer-mounted array of multiple receivers and source. In their trailer-mounted system, the receivers are mechanically lowered onto the pavement surface, and then raised before moving to the next test locations. Multi-channel analysis of surface wave (MASW) developed in the field of Geophysics overcomes the drawbacks associated with the SASW method [11–13]. In the last few years, MASW method has been further developed and applied in the scale of interest of geotechnical engineering [14–17].

This paper discusses the MASW technique for measuring shear wave velocities and for the delineation of liquefaction potential. A unified MASW analysis procedure is introduced. We attempt to provide some guidance as to the potential and limitations of the MASW method. Examples of applications come from several sites in central western Taiwan, at some of which sand boils or ground cracks occurred during 1999 Chi Chi earthquake.

2. Multi-station analysis of surface wave

Three steps are involved in a surface wave test: (1) field testing for recording surface waves, (2) determination of the experimental dispersion curve from the field data, and (3) inversion of shear wave velocity profile from the experimental dispersion curve. In the practice of SASW testing, the dispersion curve is obtained using multiple, two-receiver test configurations and the spectral analysis of the paired signals. The two-receiver configuration is sensitive to ambient noises. It has been shown that errors may arise in an experimental dispersion curve when the usual SASW test and data analysis procedure is followed, in particular the phase unwrapping procedure. Sources that contain significant energy in very low frequencies and receivers with very low natural frequencies are necessary to avoid erroneous unwrapping of phase angles. Errors at very low frequencies can severely affect the results at higher frequencies. Hence, the data acquisition system of a SASW test is typically different from that of a refraction survey although they share many things in common. Unwrapping errors may occur for sites where across the frequency range used, there is a shift from one dominant surface wave propagation mode to another, a phenomenon termed ‘mode jumping’ [18,19]. Furthermore, the use of only a pair of receivers leads to the necessity of performing the test using several testing configurations and the so-called common receiver midpoint geometry. For each receiver spacing, multiple measurements are necessary for evaluating the data coherence. This results in a quite time-consuming procedure on site for the collection of all necessary data and on data reduction for combining the dispersion data points from records obtained at all spacings. Since many non-trivial choices need to be made based on the data quality and testing configuration, the test requires the expertise of an operator and automation of the data reduction is difficult.

The coupling of multi-channel processing techniques in geophysics with smaller geotechnical engineering surveys has lead to the development of a new surveying technique, called MASW at the Kansas Geological Survey [14,15]. Methods based on multi-station data and wavefield transform are recently reported to possess several advantages for dispersion curve analysis [14–17]. Multi-station recording permits a single survey of a broad depth range, high levels of redundancy with a single field configuration, and the ability to adjust the offset, effectively reducing near field and far field effects. However, multi-station data can be analyzed in a variety of ways. Sometimes it is confusing which one should be used to obtain best results. This section introduces a unified dispersion analysis technique and describes the application of MASW in the context of investigation of liquefaction potential.

2.1. Field configuration and data acquisition

More convenient and better estimation of dispersion curve can be obtained based on a multi-station test configuration (Fig. 1), in which receivers are located at several locations along a straight line. The wavefield is discretized and truncated in both the time and space domain during the data acquisition. The sampling periods in the time and space domain are Δt and Δx; and the numbers of

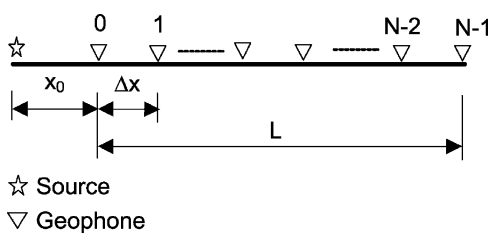

Fig. 1. A scheme of multi-station surface wave testing, in which x_0 is the near offset, Δx is the geophone spacing, and L is the offset range.

samples in the time and space domain are M and N, respectively. Modern seismographs allow very small sampling period and large number of data points in the time domain. The near offset x_0, geophone spacing Δx, and offset range L are the three important acquisition parameters that need to be properly selected, so as to prevent aliasing, near field, and far field effects. These effects determine the minimum and maximum depth in which V_S can be accurately measured by the MASW method. Because of undesirable near-field effects, Rayleigh waves can only be treated as horizontally traveling plane waves after they have propagated a certain distance from the source point. Far-offset effects arise when attenuation of high-frequency components of waves traveling along the free surface causes body waves to dominate the wavefield [14]. Furthermore, the propagating surface wave may be composed of multiple modes. Identifying individual modes requires a long offset range (L). Lin et al. [16] studied the effects of these acquisition parameters and provide some theoretical guidelines to account for the above concerns. However, the actual configuration should be decided in the field considering the space available and site conditions.

For site characterization of liquefaction potential, the depth of interest typically ranges from 2 to 20 m below the ground surface. The V_S profile obtained from a single array of surface wave test represents the average property within the geophone array. Estimates of two-dimensional (2D) velocity variations can be obtained by occupying successive array positions along a survey line. The lateral resolution depends on the length of the geophone array (L). The field testing is set out for minimizing L while maintaining the desired depth of investigation. The data processing techniques to be described below are not only useful for determining the experimental dispersion curve but also efficient for configuring field testing and data quality control.

2.2. Dispersion analysis

Multi-station tests can be analyzed using either the phase–offset regression or 2D wavefield transform methods to determine the experimental dispersion curve [16]. The phase–offset regression determines the dispersion curve based on the linear regression of phase angles measured at multiple stations. The R-square statistic (R^2) of the regression analysis serves as an index for checking the near and far field effects. The phase–offset regression method can be seen as a byproduct of the 2D wavefield transform method. Wavefield transformation methods involve a 2D wavefield transform in which the data are transformed from space–time domain into a more convenient domain. The dispersion curve is associated with the peaks in the transformed spectrum [11,12]. The frequency–slowness (f–p) transform involves first a Radon or τ–p transform on the data, followed by a one-dimensional (1D) Fourier transform along the τ direction [11]. Another method requires picking the peaks associated with surface wave energy in the frequency–wavenumber (f–k) domain from a 2D Fourier transform [12,16]. While both methods are mathematically equivalent, they have various algorithms different in resolution and efficiency. A unified algorithm for the wavefield transform is introduced herein that has high accuracy and efficiency. It is used together with the phase–offset regression method for determining the dispersion curve and on site data quality control.

The algorithm starts with a discrete Fourier transform (DFT) [20] of the multi-station data $u(t_m, x_n)$ in the time domain, resulting in DFT spectra at multiple stations.

$$U(f_i, x_n) = \frac{1}{M}\sum_{m=0}^{M-1} u(t_m, x_n)\exp(-j2\pi f_i t_m) \tag{1}$$

where u is the velocity or acceleration measured by the receiver, U is the DFT of u, $j = \sqrt{-1}$, $t_m = m\Delta t$, $f_i = i\Delta f = i/[(M-1)\Delta t]$, and $x_n = n\Delta x$. The i, n, and m in Eq. (1) are integer indices to represent, respectively, discrete points in the frequency, space, and time domain. The discretization and truncation in time domain may cause frequency aliasing and leakage in the spectral analysis [20]. The frequency aliasing can be prevented by using a sufficiently small sampling period in time (Δt) or the anti-aliasing filter in the data acquisition system such that

$$\Delta t < \frac{1}{2f_{\max}} \tag{2}$$

where $f_{\max}$ is the maximum attainable frequency of the signals. The leakage in the frequency domain does not occur when the time window $(M-1)\Delta t$ is greater than the maximum duration of the transient signals incurred by an impact source. For stationary harmonic signals, the leakage in the frequency domain is not significant if the time window $(M-1)\Delta t$ is much greater than the maximum period of the signals. Windowing technique such as the Kaiser window can be applied before the DFT to alleviate the leakage problem. The DFT is utilized for the spectral analysis because the fast Fourier transform (FFT) algorithm can be used for economically computing the transformations [20]. The frequency is also discretized in the DFT. The frequency resolution is equal to $1/[(M-1)\Delta t]$ Hz.

The amplitude spectrum of $U(f_i, x_n)$ provides information regarding the frequency content and its variation with offsets. This information is useful for adjusting test configuration on site and for determining the effective frequency range of the experimental dispersion curve. The DFT of the wavefield $u(t_m, x_n)$ with respect to time (t_m) produces $U(f_i, x_n)$ with a modulo-2π representation in the phase spectrum. The phase angle ϕ can be unwrapped in the space domain since it monotonically increases with the source-to-receiver offset x, as shown in Fig. 2 for a particular frequency f_i. In order to correctly unwrapping the phase angles in the space domain, the following criterion

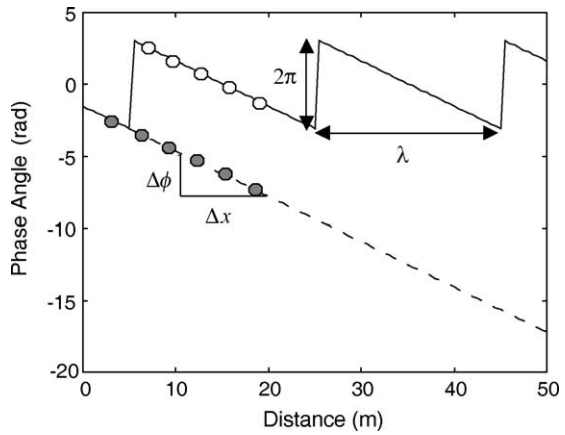

Fig. 2. An illustration of phase unwrapping in the phase–offset domain for the multi-station spectral analysis of surface wave.

should be satisfied

$$\Delta x < \frac{\lambda_{\min}}{2} \tag{3}$$

where Δx is the receiver interval and $\lambda_{\min}$ is the shortest wavelength of interest. The phase velocity (v) for each frequency f_i can then be calculated by

$$v(f_i) = \frac{2\pi f_i}{\frac{\Delta\phi}{\Delta x}} \tag{4}$$

The slope $\Delta\phi/\Delta x$ is determined by the linear regression of the unwrapped $\phi(x_n)$, as shown in Fig. 2. The data quality can be evaluated by the R-square statistic (R^2) of the regression analysis. The phase–offset regression is a multi-station extension of the SASW method, and is referred to as the multi-station spectral analysis of surface wave (MSASW) hereafter.

For each frequency component, the wavefield is a harmonic function of space. The wavenumber k (i.e. spatial frequency) can be determined from the wavenumber analysis (spectral analysis in space). The wavenumber analysis of the multi-station signals can be performed using the discrete-space Fourier transform [20]

$$Y(f_i, k) = \sum_{n=0}^{N-1} U(f_i, x_n)\exp(-j2\pi k x_n) \tag{5}$$

where $Y(f_i, k)$ represents the wavefield in the frequency–wavenumber domain. Similarly, the discretization and truncation in the space domain may cause wavenumber aliasing and leakage. Wave number aliasing can be prevented by using a $\Delta x < \lambda_{\min}$ (not $\lambda_{\min}/2$ because $U(f_i, x_n)$ is a complex number). $U(f_i, x_n)$ is a summation of harmonic functions in space according to the elastic wave propagation theory. Analogous to time-domain leakage, the measurement range in space (L) should be sufficiently long to alleviate leakage. However, this may not be possible due to limited testing space or far field effect. Windowing technique in space such as the Kaiser window can be applied before the discrete-space Fourier transform to attenuate side lobes due to leakage at the cost of increasing the main lobe width of the spectrum in the wavenumber domain.

The discrete-space Fourier transform is different from the DFT in that the wavenumber remains continuous but the fast algorithm (FFT) cannot be used. The number of stations is typically much less than the number of samples in the time domain. So the discrete-space Fourier transform rather than DFT is used in the space domain, such that the resolution in the wavenumber domain can be arbitrarily chosen. The wavenumber (k) of the surface wave can be identified at the peaks of the amplitude spectrum of $Y(f_i, k)$. The phase velocity is then determined by the definition $v = 2\pi f/k$. Spectra in other domains can be derived from Eqs. (1) and (5) by simply changing the variable $k = 2^*\pi fp$ for the frequency–slowness domain, $k = 2^*\pi f/v$ for the frequency–velocity domain, or $k = 2^*\pi/\lambda$ for the frequency–wavelength domain. For example, the frequency–velocity (f–v) transform can be obtained as

$$Y(f_i, v) = \sum_{n=0}^{N-1} U(f_i, x_n)\exp\left(-j\frac{2\pi f_i}{v}x_n\right) \tag{6}$$

where $Y(f_i, v)$ represents the wavefield in the frequency–velocity domain. Fundamental and possibly higher-mode dispersion information can be obtained by locating peaks in the f–k, f–p, f–v, or f–λ spectrum. The wavefield transform method is referred to as the multi-station wavefield transformation of surface wave (MWTSW) in this study. It is convenient to picking the dispersion curve in f–v domain since it is a direct representation of the dispersion curve in terms of velocity as a function of frequency. The f–v spectrum in the v domain is continuous so that arbitrary range and resolution can be set for data interpretation. It should be noted that the above algorithm does not require constant geophone spacing. Dead traces in the field data can be edited before performing the transformation. Energy balancing (normalization by RMS amplitudes over the full length of each trace in this case) can also be applied to account for the amplitude effects of geometrical spreading and more random differences in geophone coupling.

The phase–offset regression method is equivalent to the wavefield transform method in theory but they differ in practice. The advantages of wavefield transform method are that: (1) the phase-unwrapping procedure is completely avoided; (2) multi-mode dispersion curves may be obtained if the offset range is sufficiently long; (3) the 2D spectrum provides a good visualization for data interpretation; and (4) it is relatively insensitive to cultural noises and dead traces. The phase–offset regression method uses only the information of the phase at multiple locations. It can be seen as a byproduct of the wavefield transform method. The data quality can be evaluated and optimum offset range may be determined using the phase–offset plot. These two methods

are used collaboratively for on site data quality control and determining the dispersion curve.

2.3. Inversion analysis

The inversion of the experimental dispersion curve is based on the solution of the forward problem of Rayleigh wave propagation in a layered system. The layers are considered homogenous linear elastic; hence each of them is fully characterized by its thickness, density, and two elastic constants. To reduce the number of unknowns in the inversion process, soil density and Poisson's ratio are estimated a priori on the basis of typical values for soils and other available information.

The inversion process starts from a preliminary estimate of the shear wave velocity profile. Initial models for inversion were determined using the simple inversion formula, in which the shear wave velocity is taken as a percentage (close to 110%) of the phase velocity and assigned to a depth of 1/3–1/2 of the wavelength [9]. The profile is then adjusted to reduce the difference between the experimental and the corresponding numerical dispersion curves. This fitting process can be performed manually by trial and error (i.e. iteratively by changing the shear wave velocities from top to deeper layers), or using an automated procedure based on a nonlinear search algorithm [21–23].

The inversion analysis in this study considered only the dispersion curves associated with the fundamental mode. Higher modes may be dominant at higher frequencies. The model compatibility between the experimental and the corresponding numerical dispersion curves should be considered. Participating modes can be identified using the MWTSW analysis if the geophone array is sufficiently long [16]. Only the part associated with the fundamental mode was utilized for inversion. However, because of the short array used in geotechnical testing, it may not be possible to identify separate modes. Hence, cautions must be taken in deciding the effective frequency range of the fundamental mode if higher modes contribute significantly in the 2D spectrum.

3. Verification case

A verification case was demonstrated at a test site located at the court yard of Min Ann temple in Yuan Lin township. The soil liquefaction during Chi Chi earthquake was extensive and dramatic in this neighborhood where a water well and sections of creeks were filled up by sand following the earthquake. The soil deposit within the top 100 m at the test site consisted of mostly silty fine sand (SM), non-cohesive (ML) or low cohesive silt (CL–ML) and low cohesive sand (SC).

The experiment was set-up to gather Rayleigh waves using an array of vertical geophone (4.5 Hz). Two spreads of 24 geophones were placed roughly perpendicular to each other, one array 23 m long ($\Delta x = 1$ m) and the other 11.5 m long ($\Delta x = 0.5$ m). A sledgehammer impacting on a steel plate was used as the seismic source, which was offset 15 m from the geophone spreads. A sampling rate of 0.5 ms was used, providing a Nyquist frequency of 1000 Hz with 2048 samples recorded. Three seismic cone penetrometer tests (SCPT) were performed in a row on 2 m interval near the center of the geophone spreads.

Fig. 3 shows the results of the dispersion analysis for the short array. It is insightful to examine the surface wave data in various domains. In the time–space domain, the raw data of the shot gathers shows rich ground roll energy without much contamination of body wave or cultural noise (Fig. 3a). In the frequency–space domain, the amplitude spectrum does not show much variation with offset because of the short array used (Fig. 3b). The linearity of the phase spectrum with respect to the offset is presented as the R-square statistic (R^2) of phase–offset regression analysis as shown in Fig. 3c. Low R^2 values at low frequencies indicate the near-field effect while low values at high frequencies reveal far-field effect or mode jumping. In this case, the spectrum amplitude of high frequencies does not significantly decrease with increasing offsets. Hence, the low R^2 values at high frequencies are signs of mode jumping or multiple dominant modes rather than far field effect. Fig. 3d shows the $f-v$ spectrum and the associated (maximum) peaks at each frequency. The results of the MSASW analysis are also shown in Fig. 3d. For short geophone arrays, separate peaks associated with adjacent modes may smear or even disappear because the spectrum main lobes associated with each mode interfere with each other due to leakage in the space domain. The frequencies at which the results of MSASW and MWTSW are significantly different coincide with those frequencies with low R^2 values. The differences are due to mode jumping (i.e. the phase–offset relation becomes nonlinear) and possibly further due to unwrapping errors resulting from noise or mode jumping. The experimental dispersion curve should approach the dominant mode for long geophone arrays. For short geophone array, as is in this case, the experimental dispersion curve may not represent the 'true' answer for any modes at frequencies where multiple modes dominate. In this case, the inversion interpretation must be conducted considering the apparent phase velocity that is associated with mode superposition and the method of analysis. Since only the fundamental mode is considered in this study, the dispersion data points are excluded for analysis if the results of MWTSW are significantly different from that of MSASW. The four-plot figure as shown in Fig. 3 can be obtained on site in a fraction of seconds automatically, making it a very powerful tool for data quality control in the field. Necessary adjustments to the testing program may be made immediately after the initial test.

The results of the analysis of the adjusted geophone arrays (i.e. 23-m long array) are shown in Fig. 4. The experimental (apparent) dispersion curve becomes more

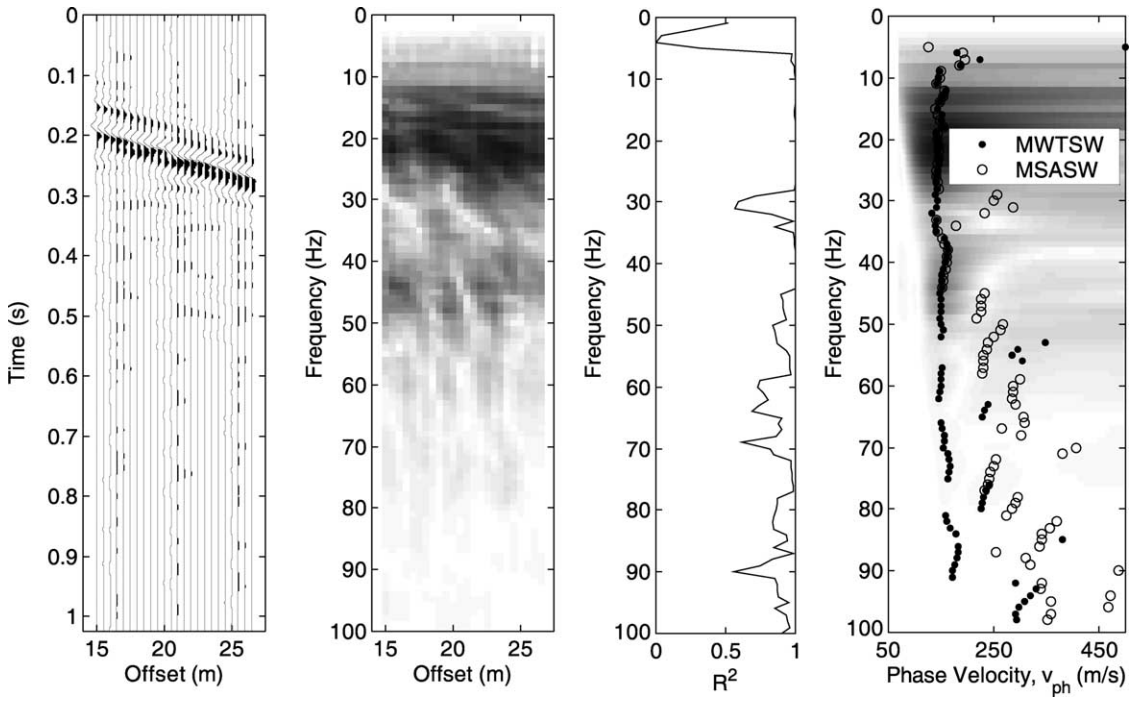

Fig. 3. Results of the dispersion analysis of the short array (11.5 m) at the verification test site: (a) raw data in the time–space domain, (b) amplitude spectrum in the frequency–space domain, (c) R^2 statistics of the linear regression in the phase–space domain, and (d) amplitude spectrum in the frequency–velocity domain.

representative of the dominant mode as the offset range increases. Furthermore, the $f-v$ spectrum clearly shows separate modes in this case. The data associated with the fundamental mode between 6 and 30 Hz was used for inversion. The final numerical dispersion curve fits the experimental one quite well as shown in Fig. 5. The nonlinear inversion was performed with the method developed by Xia et al. [21]. Fig. 6a compares the estimated

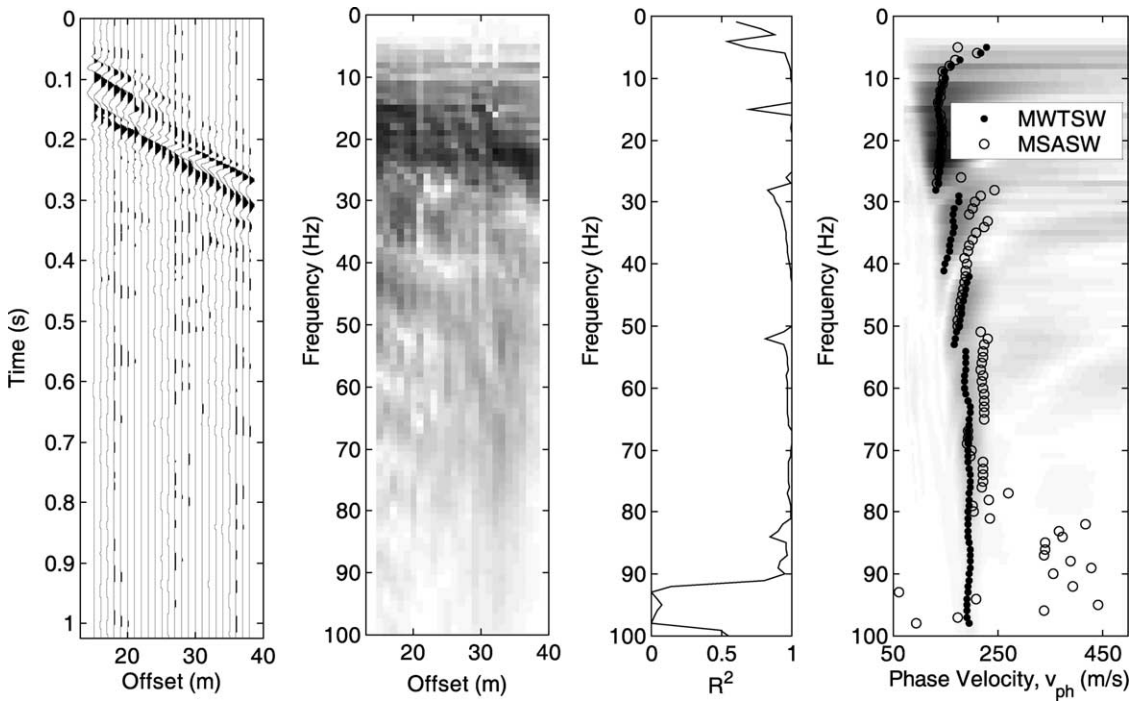

Fig. 4. Results of the dispersion analysis of the long array (23 m) at the verification test site: (a) raw data in the time–space domain, (b) amplitude spectrum in the frequency–space domain, (c) R^2 statistics of the linear regression in the phase–space domain, and (d) amplitude spectrum in the frequency–velocity domain.

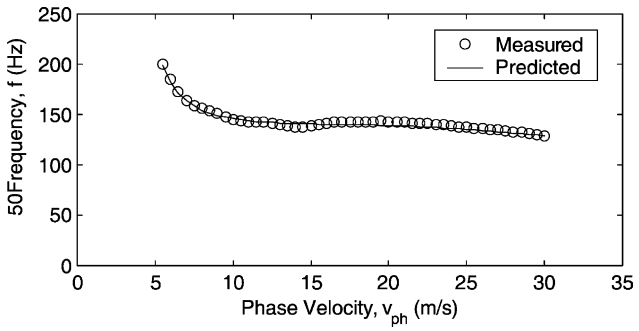

Fig. 5. Numerical dispersion curve (predicted) vs. experimental dispersion curve (measured) of the verification test site.

VS profile from the MASW test with that obtained from the SCPT tests. The MASW velocity profile shows excellent agreement with SCPT measurements. It should be noted that the shear wave velocities measured using surface wave are in the horizontal plane. These values may be in variance with those measured with downhole or seismic cone techniques if horizontal-to-vertical anisotropy exists. Furthermore, in contrast to the surface techniques, downhole methods are sensitive only to the vertical shear wave velocities and sample relatively less of the subsurface in their measurements. The penetration resistance data from CPT tests and subsequent SPT tests have indicated a rather uniform soil condition within the tested area. The fines content is about 20%. The SCPT downhole velocity profiles were calculated directly from traveltimes between adjacent points. We believe that the zigzag pattern observed in the SCPT data results from measurement errors. There is an increase in uncertainty in shear wave velocity with depth that is characteristic of both methods, especially the surface wave technique. The surface wave testing is suitable for site investigation of liquefaction potential because the target depth is mostly less than 20 m.

Using the ground motion degradation relationship by Wang et al. [24], the peak ground acceleration during Chi Chi earthquake at the test site was estimated to be 0.19 g. The ground water table was at 2.5 m below ground surface. Fig. 6b shows the FS against liquefaction following the procedure by Andrus and Stokoe [3]. Factors greater than 3 and non-liquefiable data are set to be equal to 3 in Fig. 6b. The FS was compatible with the severity of ground motion during the earthquake and the occurrence of liquefaction in this area.

4. 2D imaging of liquefaction potential

Surface wave tests were conducted in the central western Taiwan between 2001 and 2002 as part of the site characterization program for liquefaction hazard zoning in central western Taiwan. Twenty sites have been tested, in four of which liquefaction observations were reported during 1999 Chi Chi earthquake. At each site, the MASW testing was conducted following the procedure described above. Twenty-four geophones were placed in a straight line as described in Fig. 1. The geophones were constantly spaced at 1 m ($dx = 1$ m) resulting in a survey length of 23 m ($L = 23$ m) for a single test. The near offset (x_0) was adjusted in the field. Upon a round of test, the survey line was shifted in the direction of the line axis further away from first array by another 23 m and the test was repeated until a total test length of interest was completed. The total test length at each site ranges from 120 to 336 m.

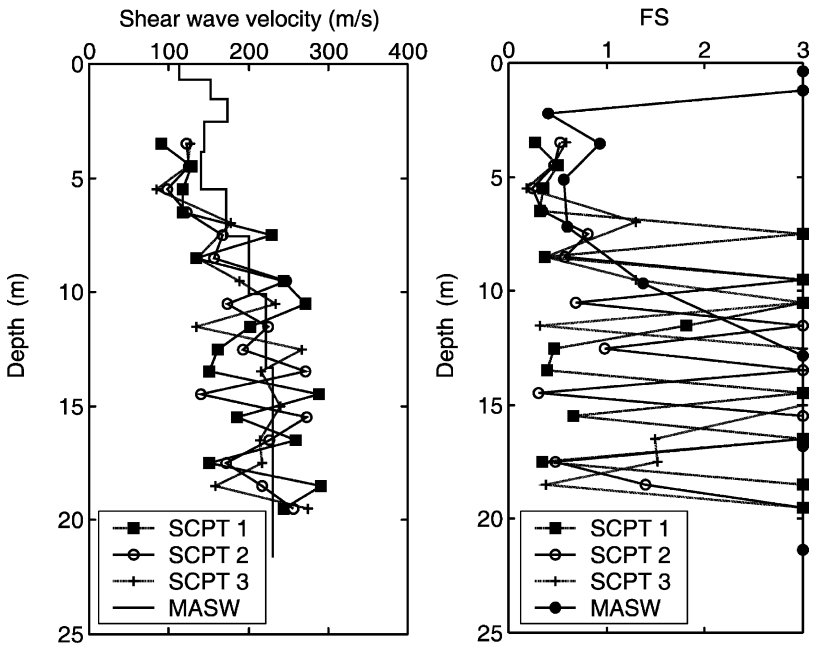

Fig. 6. Experimental results of the verification test site: (a) shear wave velocity profile, (b) FS against liquefaction.

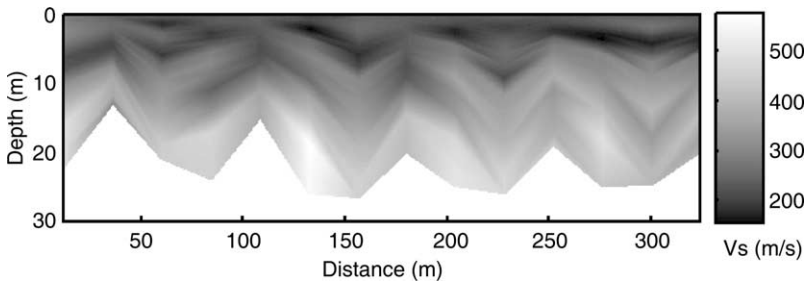

Fig. 7. Two-dimensional shear wave velocity profile from MASW.

Among the 20 sites, one is a gravelly soil where SPT and CPT tests are not feasible for evaluating liquefaction potential. The results of MASW test and liquefaction analysis are especially described below to demonstrate the advantage of non-invasive MASW test. This particular site was located on the south river bank of Da Li river, approximately 200 m west of Fu Tien bridge, in Wu Feng township of Taichung county, 4.2 km from the Chelonpu fault. Signs of soil liquefaction in forms of sand boils were observed following the earthquake. Using a ground motion degradation relationship proposed by Wang et al. [24], the geometric mean of the horizontal peak ground acceleration during Chi Chi earthquake was estimated to be 0.4 g. Soil borings performed near the test site indicated a minimum of 23 m of silt, sand and gravel mixture below the ground surface. Most SPT performed in the gravel layer were terminated when the blow counts exceeded 50 before reaching 15 cm of penetration. The ground water table was at 3.5 m below the ground surface.

The MASW analysis of the test data provided a 2D V_S profile as shown in Fig. 7. The effective depth of measurement was approximately 20 m, and the total length of measurement was 322 m with fourteen 23-m segments of MASW tests. Linear interpolation was used to present the shear wave velocity profile in 2D. Factor of safety against liquefaction was estimated following the method by Andrus and Stokoe [3] for clean sand. A 2D FS profile are shown in Fig. 8. The limiting shear wave velocity V_{S1}^{*} was assumed to be 215 m/s, beyond which the soil was considered non-liquefiable and the FS was assigned to be 2.0 in Fig. 8. Liquefiable layers or pockets at depths between 4 and 7 m, comparable with results of large penetration tests reported elsewhere [25]. The results of liquefaction potential assessments were consistent with the signs of soil liquefaction observed at the test site following the Chi Chi earthquake. It should be noted that the liquefaction potential assessments were made using the method for clean sand. The effects of gradation or fines content in the simplified procedure were not considered. However, considering the many uncertainties in estimating the cyclic stress ratio and cyclic resistance ratio (CRR) in the simplified procedure, the above analysis still provides insightful and valuable information about the site. The MASW imaging is an expedient and cost-effective technique; it is effective for estimating the extent of potential liquefaction hazard. Further detailed investigation or ground improvement can then be planned accordingly.

Among the 20 surface wave imaging tests, the four sites in which liquefactions were observed during the Chi Chi earthquake and three of the 16 non-liquefied sites shows liquefaction susceptibility based the method by Andrus and Stokoe [3]. The simplified analysis may be too conservative when using the shear wave velocity for liquefaction potential analysis. The CRR limit state curve reported in Andrus and Stokoe [3] tried to encompass all the liquefied data in the liquefiable side, leaving some non-liquefied cases also in the liquefiable side. These non-liquefied cases are mostly associated with soils with fines content greater than 35%. Considering the granular deposits in central western Taiwan are characteristic of high fines content. The results of liquefaction potential analysis based on MASW test are quite reasonable.

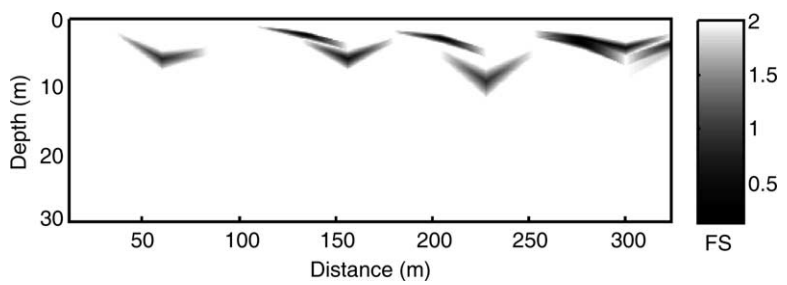

Fig. 8. Two-dimensional profile of the factor of safety from MASW.

5. Conclusions

The MASW method is a non-invasive seismic approach to estimate shear wave velocity profile from surface wave energy. This paper discusses the MASW technique for measuring near-surface shear wave velocities, and for the delineation of liquefaction potential in 2D. MASW can be performed in a variety of ways; it is often confusing which one should be used to obtain best results. A unified dispersion analysis technique is introduced in this study using discrete Fourier transform (FFT) in the time domain and discrete-space Fourier transform in the space domain. This technique is also a powerful tool for on site quality control in real time.

A verification case demonstrates the procedure of MASW analysis and the results are compared with that of SCPT. The MASW velocity profile shows excellent agreement with SCPT measurements. 2D imaging of S-wave velocities were conducted at several sites in central western Taiwan, at some of which sand boils or ground cracks occurred during 1999 Chi Chi earthquake. The results of liquefaction potential assessments using MASW data were consistent with the signs of soil liquefaction observed following the Chi Chi earthquake.

The MASW test is non-invasive, expedient, and cost effective. It can be used to produce a single 1D V_S profile or a 2D V_S profile that covers a wide range of area. Liquefaction potential analysis based on MASW imaging is effective for estimating the extent of potential liquefaction hazard, so as to justify further detailed investigation or ground improvement plan.

Two-receiver configuration of the surface wave testing is theoretically a special case of the multi-station method. While SASW uses a phase difference method to determine the phase velocity, the MASW permits the use of a 2D wavefield transformation in addition to the phase difference method. The determination of dispersion curve using multi-station recordings and the 2D wavefield transformation has several advantages: (1) field testing is more efficient; (2) common refraction equipment can be used; (3) it permits implementation of a robust automation algorithm; (4) it is free from unwrapping error; (5) it is much more insensitive to ambient noises; (6) analysis of higher modes is possible. The MASW typically involves just one source location. Problems that may arise from just one source location involve the attenuation of high frequencies, which cannot be adequately determined at the far receiver spacings. Traditional SASW has the merit of involving multiple two-receiver spacings and source locations to ensure that dispersion curve is adequately characterized at both low and high frequencies. However, when both near surface and deep layers are of interest, the MASW can also accommodate multiple sources with different near offsets and energies and the appropriate offset range is selected for the dispersion analysis. It should be noted that accurate characterization of near surface layers involves not only having high frequency component but also taking into account multiple modes. Improvement of the vertical resolution and inversion considering model compatibility for multiple modes or offset-dependent apparent velocities are currently under investigation. Traditional SASW involves using multiple, two-receiver set-ups about a centerline to determine the best dispersion curve around a common midpoint. The dispersion curve determined from the MASW represents the average value beneath the geophone spread. Research is also underway to reduce the length of the geophone spread so that the lateral variations of shear wave structure can be mapped out with much higher spatial resolution.

Acknowledgements

Funding for this research was provided by the National Science Council of ROC under contracts No. 89-2218-E-009-101 and 90-2611-E009-003. The manuscript has been improved by the helpful comments and suggestions of two anonymous reviewers.

References

[1] Youd TL, Idriss IM, Andrus RD, Arango I, Castro G, Christian JT, Dobry R, Finn L, Harder Jr LF, Hynes ME, Ishihara K, Koester JP, Liao S, Marcuson III WF, Martin GR, Mitchell JK, Moriwaki Y, Power MS, Robertson PK, Seed RB, Stokoe II KH. Liquefaction resistance of soils: summary report from the 1996 NCEER and 1998 NCEER/NSF workshops on evaluation of liquefaction resistance of soils. J Geotech Geoenv Eng 2001;127(10):817–33.

[2] Tokimatsu K, Uchida A. Correlation between liquefaction resistance and shear wave velocity. Soils Found 1990;30(2):33–42.

[3] Andrus RD, Stokoe II KH. Liquefaction resistance of soils from shear-wave velocity. J Geotech Geoenv Eng 2000;126(11):1015–25.

[4] Palmer D. In: Helbig K, Treitel S, editors. Refraction seismics, the lateral resolution of structure and seismic velocity. The handbook of geophysical exploration, section I, vol. 13. London: Geophys Press; 1986.

[5] Pullammanappallil SK, Louie JN. A generalized simulated-annealing optimization for inversion of first arrival times. Bull Seismo Soc Am. 1994;84(5):1397–409.

[6] Xia J, Miller RD, Park CB. A pitfall in shallow shear-wave refraction surveying. SEG, 69th Annual Meeting, Houston, TX; 1999. p. 508–11.

[7] Nazarian S, Stokoe II KH. In situ shear wave velocities from spectral analysis of surface waves. Proceedings of Eighth Conference on Earthquake Engineering, San Francisco, vol. 3; 1984. p. 38–45.

[8] Stokoe II KH, Nazarian S, Rix GJ, Sanchez-Salinero I, Sheu J, Mok Y. In situ seismic testing of hard-to-sample soils by surface wave method. Earthquake engineering and soil dynamics II—recent advances in ground motion evaluation, Geotechnical Special Publication No. 20; 1988. p. 264–277.

[9] Stokoe II KH, Wright GW, Bay JA, Roesset JM. Characterization of geotechnical sites by SASW method. In: Woods ED, editor. Geophysical characterization of sites. Rotterdam: A.A. Balkema; 1994. p. 15–25.

[10] Nazarian S, Yuan D, Baker MR. Rapid determination of pavement moduli with spectral-analysis-of-surface-waves method. Research Report 1243-1, Center for Geotechnical and Highway Materials Research, University of Texas at El Paso.

[11] McMechan GA, Yedlin MJ. Analysis of dispersive waves by wave field transformation. Geophysics 1981;46:869–74.
[12] Gabriels P, Snieder R, Nolet G. In situ measurements of shear-wave velocity in sediments with higher-mode Rayleigh waves. Geophysical Prospecting 1987;35:187–96.
[13] Park CB, Miller RD, Xia J. Imaging dispersion curves of surface waves on multi-channel record. 68th Annual International Meeting, Society of Exploration Geophysicists, Expanded Abstracts. 1998. p. 1377–80.
[14] Park CB, Miller RD, Xia J. Multichannel analysis of surface waves. Geophysics 1999;64(3):800–8.
[15] Xia J, Miller RD, Park CB, Hunter JA, Harris JB, Ivanov J. Comparing shear-wave velocity profiles inverted from multichannel surface wave with borehole measurements. Soil Dyn Earthquake Eng 2002;22: 181–90.
[16] Lin CP, Chang TS, Cheng MH. Shear-wave velocities from multi-station analysis of surface wave. Proceedings of the Third International Symposium on Deformation Characteristics of Geomaterials, Lyon, France; 2003. p. 1335–43.
[17] Foti S, Fahey M. Applications of multistation surface wave testing. Proceedings of the Third International Symposium on Deformation Characteristics of Geomaterials, Lyon, France; 2003. p. 13–19.
[18] Al-Hunaid MO. Difficulties with phase spectrum unwrapping in SASW nondestructive testing of pavements. Can Geotech J 1992;29: 506–11.
[19] Tokimatsu K, Tamura S, Kojima H. Effects of multiple modes on Rayleigh wave dispersion characteristics. J Geotech Eng 1992; 118(10):1529–43.
[20] Prokis JG, Manolakis DG. Digital signal processing-principles, algorithms, and applications, 3rd ed. New Jersey: Prentice Hall; 1992.
[21] Xia J, Miller RD, Park CB. Estimation of near-surface shear-wave velocity by inversion of Rayleigh waves. Geophysics 1999;64: 691–700.
[22] Herrmann RB. Computer programs in seismology, ver. 3.20. Missouri: Saint Louis University; 2002.
[23] Rosset JM, Chang DW, Stokoe II KH. Comparison of 2-D and 3-D models for analysis of surface wave tests. Proceedings of Fifth International Conference on Soil Dynamics and Earthquake Engineering, Karlsruhe, Germany; 1991. p. 111–26.
[24] Wang GQ, Zhou XY, Zhang PZ, Igel H. Characteristics of amplitude and duration for near fault strong ground motion from the 1999 Chi-Chi, Taiwan earthquake. Soil Dyn Earthquake Eng 2002;73–96.
[25] Huang AB, Lee DH, Lin PS, Tsai JS, Lin CP, Chi YY, Ku CS, Chen JW, Juang CH, Liou YJ. Lessons learned from the post Chi Chi EQ geotechnical explorations in central western Taiwan. Proceedings of the 12th Pan American Conference on Soil Mechanics and Geotechnical Engineering, Cambridge, Massachusetts, vol. 1; 2003. p. 245–52.